PROCEEDINGS OF SPIE

Applications of Digital Image Processing XLIII

Andrew G. Tescher
Touradj Ebrahimi
Editors

24 August – 4 September 2020
Online Only, United States

Sponsored and Published by
SPIE

Volume 11510

Part One of Two Parts

Proceedings of SPIE 0277-786X, V. 11510

Applications of Digital Image Processing XLIII, edited by Andrew G. Tescher,
Touradj Ebrahimi, Proc. of SPIE Vol. 11510, 1151001 · © 2020 SPIE
CCC code: 0277-786X/20/$21 · doi: 10.1117/12.2581642

The papers in this volume were part of the technical conference cited on the cover and title page. Papers were selected and subject to review by the editors and conference program committee. Some conference presentations may not be available for publication. Additional papers and presentation recordings may be available online in the SPIE Digital Library at SPIEDigitalLibrary.org.

The papers reflect the work and thoughts of the authors and are published herein as submitted. The publisher is not responsible for the validity of the information or for any outcomes resulting from reliance thereon.

Please use the following format to cite material from these proceedings:
Author(s), "Title of Paper," in *Applications of Digital Image Processing XLIII*, edited by Andrew G. Tescher, Touradj Ebrahimi, Proceedings of SPIE Vol. 11510 (SPIE, Bellingham, WA, 2020) Seven-digit Article CID Number.

ISSN: 0277-786X
ISSN: 1996-756X (electronic)

ISBN: 9781510638266
ISBN: 9781510638273 (electronic)

Published by
SPIE
P.O. Box 10, Bellingham, Washington 98227-0010 USA
Telephone +1 360 676 3290 (Pacific Time) · Fax +1 360 647 1445
SPIE.org

Printed in the United States of America by Curran Associates, Inc., under license from SPIE.

Publication of record for individual papers is online in the SPIE Digital Library.

SPIE. DIGITAL LIBRARY
SPIEDigitalLibrary.org

Paper Numbering: *Proceedings of SPIE* follow an e-First publication model. A unique citation identifier (CID) number is assigned to each article at the time of publication. Utilization of CIDs allows articles to be fully citable as soon as they are published online, and connects the same identifier to all online and print versions of the publication. SPIE uses a seven-digit CID article numbering system structured as follows:

- The first five digits correspond to the SPIE volume number.
- The last two digits indicate publication order within the volume using a Base 36 numbering system employing both numerals and letters. These two-number sets start with 00, 01, 02, 03, 04, 05, 06, 07, 08, 09, 0A, 0B … 0Z, followed by 10-1Z, 20-2Z, etc. The CID Number appears on each page of the manuscript.

Diffuse tomography of brain nerve tissue in the temporary monitoring of pathological changes in optical anisotropy

Garazdyuk, M., Vanchulyak, O., Zavolovich, Y., Tomka, Y., Soltys, I., et al.

M. Garazdyuk, O. Vanchulyak, Y. Zavolovich, Y. Tomka, I. Soltys, O. Dubolazov, V. Dvorjak, "Diffuse tomography of brain nerve tissue in the temporary monitoring of pathological changes in optical anisotropy," Proc. SPIE 11510, Applications of Digital Image Processing XLIII, 115102Q (21 August 2020); doi: 10.1117/12.2568443

SPIE.

Event: SPIE Optical Engineering + Applications, 2020, Online Only

Diffuse tomography of brain nerve tissue in the temporary monitoring of pathological changes in optical anisotropy

M.Garazdyuk[1], O.Vanchulyak[1], Y. Zavolovich[1], Yu. Tomka[2], I. Soltys[2], O. Dubolazov[2], V. Dvorjak[2]

[1] Bukovinian State Medical University, 3 Theatral Sq., Chernivtsi, Ukraine, 58000
[2] Chernivtsi National University, 2 Kotsiubynskyi Str., Chernivtsi, Ukraine, 58012

a.dubolazov@chnu.edu.ua

ABSTRACT

1. Development of a structural-logical scheme and experimental testing of methods and means of diffuse tomography new in forensic practice for reproducing fluctuations in the magnitude of linear and circular birefringence and dichroism of the polycrystalline structure of histological sections of the brain.
2. Experimental determination of a set of maps and histograms fluctuation distributions of linear (FFLB) and circular (FFCB) birefringence and dichroism (FALD and FACD) for differential diagnosis of traumatic hemorrhage, cerebral infarction ischemic and hemorrhagic genesis using diffuse tomography of polycrystalline structure of histological sections of the brain.
3. Information analysis to determine the operational characteristics of the force (sensitivity, specificity and balanced accuracy) of the diffuse tomography method.

Keywords: diffuse tomography, anisotropy, brain nerve tissue, diagnostics.

1. DIFFERENTIAL DIAGNOSIS OF THE FORMATION OF HEMORRHAGES OF TRAUMATIC GENESIS, CEREBRAL INFARCTION OF ISCHEMIC AND HEMORRHAGIC GENESIS USING MUELLER-MATRIX MICROSCOPY

1.1. Azimuthally invariant Mueller-matrix images of the optical activity of histological sections of the brain.

The results of the study of the coordinate distributions of the Mueller-matrix invariant of circular birefringence (MMI OA) of protein complexes of the nervous tissue of samples of histological sections of the brain of dead from various groups are presented in a series of fragments of fig.1[1-4].

Applications of Digital Image Processing XLIII, edited by Andrew G. Tescher, Touradj Ebrahimi, Proc. of SPIE Vol. 11510, 115102Q · © 2020 SPIE
CCC code: 0277-786X/20/$21 · doi: 10.1117/12.2568443

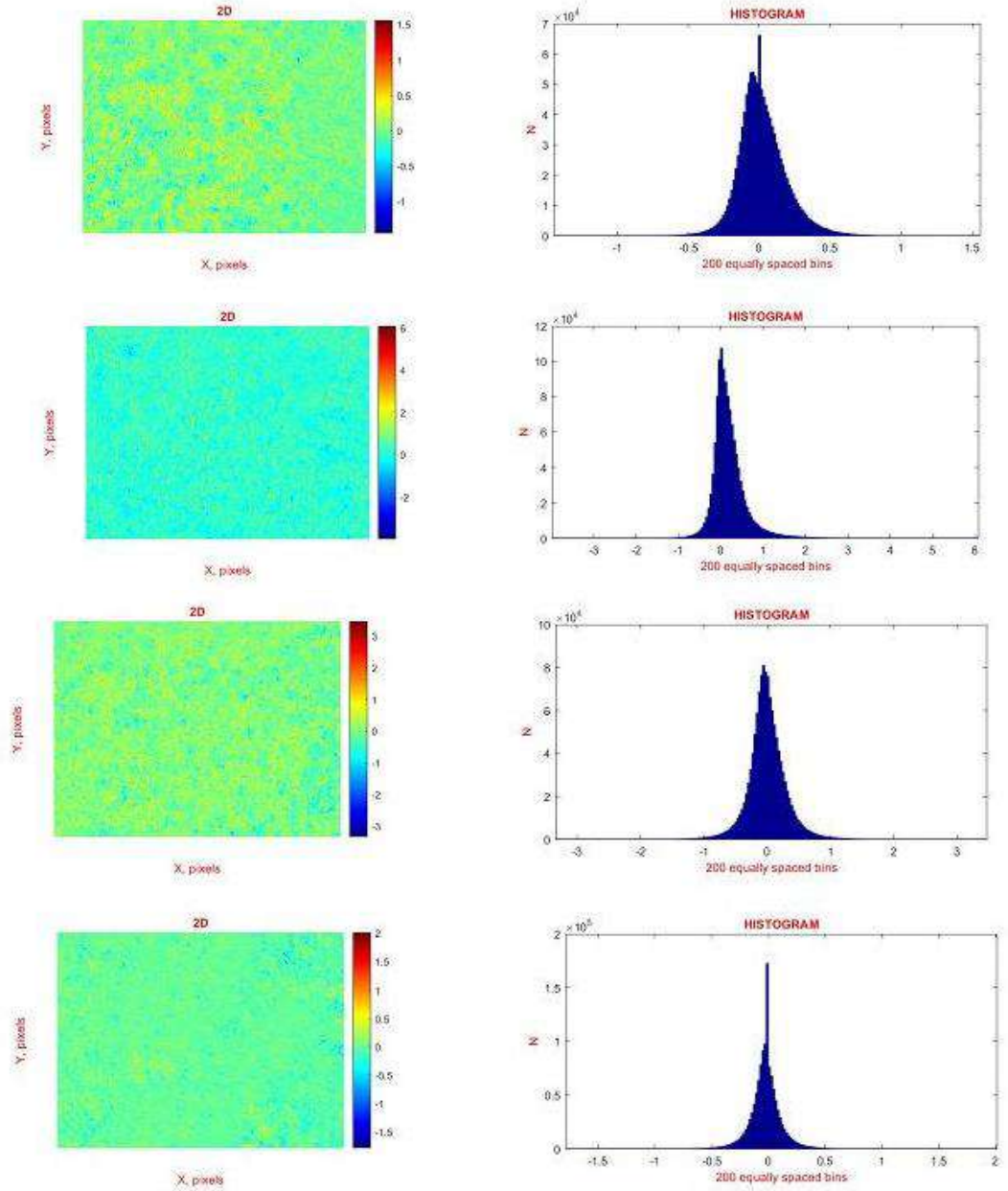

Fig. 1. Maps ((1), (2), (3), (4)) and histograms ((4), (5), (6), (7)) the distribution of the MMI OA of histological sections of the brain of the dead from group 1 ((1), (5)), group 2 ((2), (6)), group 3 ((3), (7)) and group 4 ((4), (8)).

From the analysis of the data obtained by Mueller-matrix mapping of polarization manifestations of optical activity[5-9]:

- more homogeneous, in comparison with the results of the polarimetry of the distributions of the OP values and PP, the coordinate-inhomogeneous structure of all MMI OA maps of histological sections of the brain of nervous tissue of deceased from all groups (fig. 1, fragments (1) , (3), (5), (7));

- for histograms characterizing the MMI maps of samples from all (control 1 and research 2 - 4) groups, a small scatter of values (dispersion), significant asymmetry (), and sharpness (excess) of the peak (Fig. 1, fragments (2), (4), (6), (8));

- the difference in the statistical structure of the coordinate distributions of the magnitude of the MMI OA of histological sections of the brain of the dead from control group 1 and all research groups 2 - 4 - (Fig. 1, fragment (1) and fragments (4),(6),(8)).

Table 1 presents the average values and errors ($\pm\Omega$) determination of the set of statistical moments of the 1st - 4th orders $SM_{i=1-4}$ that characterize the Mueller-matrix images of the polarization of the manifestations of the circular birefringence of optically active protein complexes of the nervous tissue of the brain.

A comparative analysis with the data of statistical analysis of laser microscopic polarimetry of the distributions of the OP and PP values of digital microscopic images of histological sections of the brain revealed the diagnostic sensitivity of statistical moments of the 3rd and 4th orders (highlighted in green - table 1) for azimuthally invariant Mueller-matrix differentiation of brain nerve tissue samples of the dead from control group 1 and all research groups 2 - 4 (p_1 p 0,05).

Intergroup (research groups 2–4) differences between the coordinate divisions of the MMI OA of the research representative samples of histological sections of the brain were also statistically unreliable - $p_{i=2;3;4}$ f 0,05 .

Table 1. Statistical moments of the 1st - 4th orders characterizing the distribution of the magnitude of the MMI OA of histological sections of the brain of groups 1 – 4

Parameters	Group 1	Group 2	Group 3	Group 4
SM_1	0,21 ± 0,009	0,19 ± 0,008	0,17 ± 0,007	0,18 ± 0,008
p_1		p ϕ 0,05	p ϕ 0,05	p ϕ 0,05
p_2		p ϕ 0,05		p ϕ 0,05
p_3		p ϕ 0,05	p ϕ 0,05	
p_4		p ϕ 0,05		
SM_2	0,17 ± 0,007	0,21 ± 0,009	0,18 ± 0,008	0,14 ± 0,006
p_1		p ϕ 0,05	p ϕ 0,05	p ϕ 0,05
p_2		p ϕ 0,05		p ϕ 0,05
p_3		p ϕ 0,05	p ϕ 0,05	
p_4		p ϕ 0,05		
SM_3	0,59 ± 0,026	0,71 ± 0,031	0,81 ± 0,037	0,88 ± 0,039
p_1		p p 0,05	p p 0,05	p p 0,05
p_2		p ϕ 0,05		p f 0,05
p_3		p ϕ 0,05	p f 0,05	
p_4		p f 0,05		
SM_4	2,51 ± 0,11	3,11 ± 0,14	3,36 ± 0,15	4,01 ± 0,18
p_1		p p 0,05	p p 0,05	p p 0,05
p_2		p ϕ 0,05		p ϕ 0,05
p_3		p f 0,05	p f 0,05	
p_4		p f 0,05		

1.2. Operational characteristics of the method of statistical analysis of maps of MMI OA of histological sections of the brain.

A certain increase in the diagnostic efficiency and strength of the method of microscopic azimuthally invariant Mueller-matrix polarimetry of the distributions of the values of MMI OA for objective statistical differentiation of the causes of death is illustrated by the values of the set of operational characteristics (sensitivity, specificity and balanced accuracy), which are shown in table 2.

Table 2. The specificity, sensitivity, accuracy of the method of statistical analysis of maps of MMI OA of histological sections of the brain

Groups "1 – 2+3+4"			
Parameters	Sensitivity, Se,%	Specificity, Sp,%	Accuracy, Ac,%
SM_1	$a=63; b=37$	$c=61; d=39$	$n=100$
	63	**61**	**62**
SM_2	$a=61; b=39$	$c=60; d=40$	$n=100$
	61	**60**	**60,5**
SM_3	$a=77; b=23$	$c=75; d=25$	$n=100$
	77	**75**	**76**
SM_4	$a=73; b=27$	$c=71; d=29$	$n=100$
	73	**71**	**72**
Groups "2 – 3"			
Parameters	Sensitivity, Se,%	Specificity, Sp,%	Accuracy, Ac,%
SM_1	$a=62; b=38$	$c=61; d=39$	$n=100$
	62	**61**	**61,5**
SM_2	$a=61; b=39$	$c=61; d=39$	$n=100$
	61	**61**	**61**
SM_3	$a=65; b=35$	$c=63; d=37$	$n=100$
	65	**63**	**64**
SM_4	$a=63; b=37$	$c=61; d=39$	$n=100$
	63	**61**	**62**
Groups "2 – 4"			
Parameters	Sensitivity, Se,%	Specificity, Sp,%	Accuracy, Ac,%
SM_1	$a=63; b=37$	$c=61; d=39$	$n=100$
	63	**61**	**62**
SM_2	$a=62; b=38$	$c=61; d=39$	$n=100$
	62	**61**	**61,5**
SM_3	$a=66; b=34$	$c=64; d=36$	$n=100$
	66	**64**	**65**
SM_4	$a=65; b=35$	$c=64; d=36$	$n=100$
	65	**64**	**64,5**
Groups "3 – 4"			
Parameters	Sensitivity, Se,%	Specificity, Sp,%	Accuracy, Ac,%
SM_1	$a=62; b=38$	$c=61; d=39$	$n=100$
	62	**61**	**61,5**
SM_2	$a=61; b=39$	$c=61; d=39$	$n=100$
	61	**61**	**61**
SM_3	$a=63; b=37$	$c=61; d=39$	$n=100$
	63	**61**	**62**

SM_4	$a = 63; b = 37$	$c = 60; d = 40$	$n = 100$
	63	**60**	**61,5**

For each of the 1st-4th-order statistical moments that characterize the MMI OA maps of circularly birefringent protein complexes of histological sections of the brain of deceased from all groups, the sensitivity $Se,\%$, specificity $Sp,\%$ and balanced accuracy $Ac,\%$ increase by 10% -15% compared with direct data polarization mapping[10-15].

For a third-order statistical moment, which characterizes the asymmetry of the distributions of the MMI OA, the strength of the Mueller-matrix microscopy method in the differentiation of samples from the control and experimental groups reaches a satisfactory level – 75% - 77%.

1.3. Azimuthally invariant Mueller-matrix images of linear birefringence of histological sections of the brain.

In fig. 2 shows the results of the azimuthally invariant Mueller matrix mapping of maps (fragments (1), (3), (5), (7)) and histograms of the distribution of magnitude (fragments (2), (4), (6), (8)) MMI LB, characterizing the polarization manifestations of linear birefringence of the fibrillar networks of the brain nervous tissue of the dead from groups 1-4.

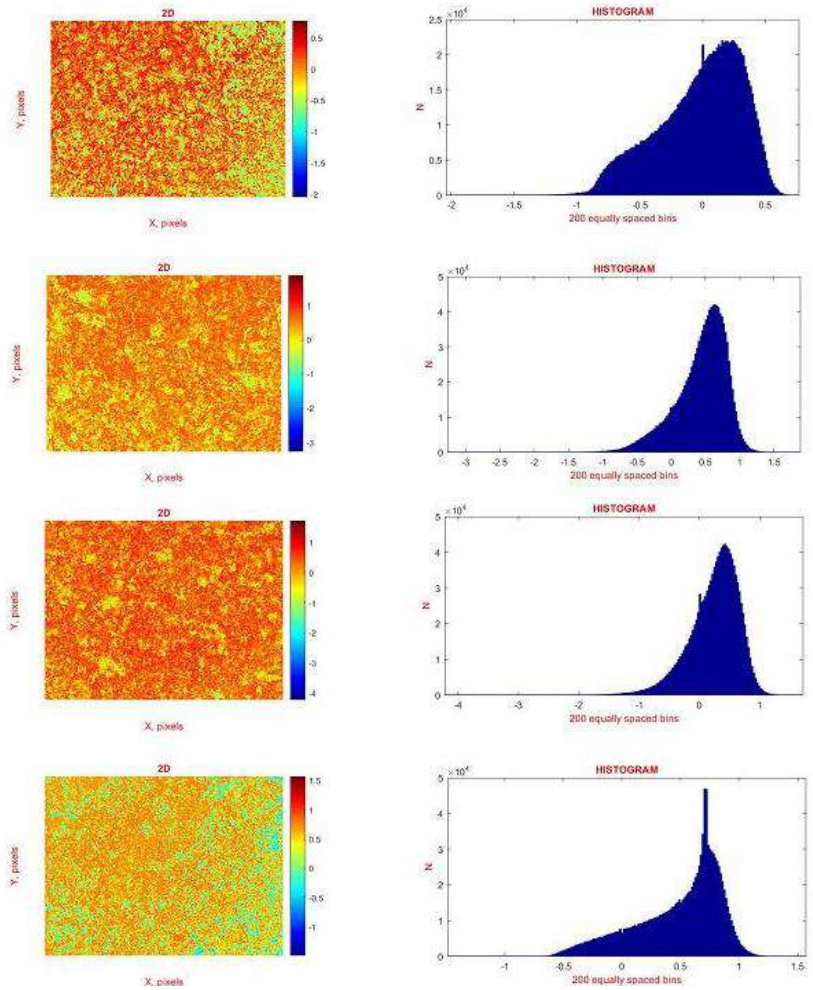

Fig. 2. Maps ((1), (2), (3), (4)) and histograms ((4), (5), (6), (7)) the distribution of the MMI of the LD of histological sections of the brain of the dead from group 1 ((1), (5)), group 2 ((2), (6)), group 3 ((3), (7)) and group 4 ((4), (8)).

A comparative analysis of the results of Mueller-matrix mapping of polarization manifestations of linear birefringence of fibrillar networks of brain samples was found:

- significant, in comparison with the results of polarimetric distributions of the values of OP and PP and MMI OA (fig. 1), coordinate-heterogeneous heterogeneity of the MMI LB maps of histological sections of the brain tissue of the dead of all groups (fig. 2, fragments (1), (3), (5), (7));
- histograms characterizing the distribution of the MMI LB value of samples from all (control 1 and research 2 - 4) groups are characterized by individual and significant scatter of values (dispersion SM_2), asymmetry (SM_3) and peak acuity (excess SM_4) (Fig. 2, fragments (2), (4), (6), (8))
- the difference in the statistical structure of the coordinate distributions of the magnitude of the MMI LB of histological sections of the nervous tissue of the brain of the dead not only from the control group 1 and all research groups 2 - 4 - (fig. 2, fragment (1) and fragments (4), (6), (8)), but also within the intergroup limits - "group 2 - group 4" and "group 2 and group 3"

Table 3 shows the data of statistical analysis of the maps of MMI LB of the brain nervous tissue.

Table 3. Statistical moments of the 1st - 4th orders characterizing the distribution of the value of MMI LB histological sections of the brain of groups 1 – 4

Parameters	Group 1	Group 2	Group 3	Group 4
SM_1	0,21 ± 0,009	0,24 ± 0,011	0,23 ± 0,01	0,19 ± 0,008
p_1		p π 0,05	p π 0,05	p π 0,05
p_2		p ϕ 0,05		p ϕ 0,05
p_3		p ϕ 0,05	p ϕ 0,05	
p_4		p ϕ 0,05		
SM_2	0,24 ± 0,011	0,37 ± 0,017	0,35 ± 0,016	0,31 ± 0,014
p_1		p π 0,05	p π 0,05	p π 0,05
p_2		p ϕ 0,05		p ϕ 0,05
p_3		p ϕ 0,05	p ϕ 0,05	
p_4		p ϕ 0,05		
SM_3	0,61 ± 0,027	0,75 ± 0,034	0,78 ± 0,035	0,91 ± 0,044
p_1		p π 0,05	p π 0,05	p π 0,05
p_2		p ϕ 0,05		p π 0,05
p_3		p ϕ 0,05	p ϕ 0,05	
p_4		p ϕ 0,05		
SM_4	0,87 ± 0,041	1,02 ± 0,048	1,12 ± 0,051	1,32 ± 0,059
p_1		p π 0,05	p π 0,05	p π 0,05
p_2		p ϕ 0,05		p ϕ 0,05
p_3		p ϕ 0,05	p ϕ 0,05	
p_4		p ϕ 0,05		

A comparative analysis with the data of statistical analysis of laser microscopic polarimetry of the distributions of the OP and PP values of digital microscopic images and MMI OA of histological sections of the brain, presented in table 1, showed the diagnostic sensitivity of statistical moments of the 2nd - 4th orders (highlighted in green - table 3) for microscopic azimuthally invariant Mueller-matrix differentiation of the manifestations of linear birefringence of fibrillar networks of brain nerve tissue samples of the dead from the control group 1 and all the groups 2 - 4 (p_1 p 0,05). In addition, the possibility of intergroup (research groups 2–4) statistical differentiation of the coordinate distributions of the magnitude of the MMI LB of representative samples of histological sections of the brain − group 2 − group 4 "(p_3 p 0,05) and" group 2 and group 3 "(p_2 p 0,05) was revealed.

1. 4. Operational characteristics of the method of statistical analysis of maps MMI LB histological sections of the brain.

A significant increase in the operational characteristics characterizing the strength of the method of microscopic azimuthally invariant Mueller-matrix polarimetry of the distributions of the MMI LB of brain nerve tissue samples for objective statistical differentiation of the causes of death illustrate the sensitivity, specificity and balanced accuracy values shown in table 4.

For each set of statistical moments 1–4 orders of magnitude, which characterize the coordinate distributions of the magnitude of the MMI LB of the fibrillar networks of the nervous tissue of samples of histological sections of the brain of deceased from all groups, the sensitivity $Se,\%$, specificity $Sp,\%$ and balanced accuracy increase $Ac,\%$ by 12% – 18% in compared with the data of Mueller-matrix mapping of polarization manifestations of the optical activity of protein complexes (table 2).

For statistical moments of the 1st, 3rd and 4th orders characterizing the distribution of the MMI LB, the strength of the Mueller-matrix microscopy method in the differentiation of samples from the control and experimental groups reaches a satisfactory level – 75% - 85%.

Table 4. The specificity, sensitivity, accuracy of the method of statistical analysis of maps MMI LB of histological sections of the brain

Groups "1 – 2+3+4"			
Parameters	Sensitivity, $Se,\%$	Specificity, $Sp,\%$	Accuracy, $Ac,\%$
SM_1	$a=77; b=23$	$c=75; d=25$	$n=100$
	77	**75**	**76**
SM_2	$a=72; b=28$	$c=69; d=31$	$n=100$
	72	**69**	**71**
SM_3	$a=82; b=18$	$c=79; d=21$	$n=100$
	82	**79**	**81**
SM_4	$a=85; b=15$	$c=81; d=19$	$n=100$
	85	**81**	**83**
Groups "2 – 3"			
Parameters	Sensitivity, $Se,\%$	Specificity, $Sp,\%$	Accuracy, $Ac,\%$
SM_1	$a=66; b=34$	$c=64; d=36$	$n=100$
	66	**64**	**65**
SM_2	$a=68; b=32$	$c=65; d=35$	$n=100$
	68	**65**	**66,5**
SM_3	$a=80; b=20$	$c=76; d=24$	$n=100$
	80	**76**	**78**
SM_4	$a=81; b=19$	$c=77; d=23$	$n=100$
	81	**77**	**79,5**
Groups "2 – 4"			
Parameters	Sensitivity, $Se,\%$	Specificity, $Sp,\%$	Accuracy, $Ac,\%$
SM_1	$a=63; b=37$	$c=60; d=40$	$n=100$
	63	**60**	**61,5**
SM_2	$a=65; b=35$	$c=62; d=38$	$n=100$
	65	**62**	**63,5**
SM_3	$a=78; b=22$	$c=75; d=25$	$n=100$

	78	**75**	**76,5**
SM_4	$a=79; b=21$	$c=77; d=23$	$n=100$
	79	**77**	**78**
Groups "3 – 4"			
Parameters	Sensitivity, $Se,\%$	Specificity, $Sp,\%$	Accuracy, $Ac,\%$
SM_1	$a=61; b=39$	$c=60; d=40$	$n=100$
	61	**60**	**60,5**
SM_2	$a=63; b=37$	$c=61; d=39$	$n=100$
	63	**61**	**62**
SM_3	$a=66; b=34$	$c=63; d=37$	$n=100$
	66	**63**	**64,5**
SM_4	$a=70; b=30$	$c=66; d=34$	$n=100$
	70	**66**	**68**

CONCLUSIONS

The effectiveness between the group differentiation of samples of deaths from traumatic hemorrhage (group 2) and ischemic cerebral infarction (group 3) reaches a satisfactory level and is 77% - 81%.

A similar (satisfactory - 75% - 79%) level of differentiation corresponds to the diagnostic capabilities of MMI LB microscopy of samples of patients who died from hemorrhagic (group 4) and ischemic cerebral infarction (group 3).

For control group 1 (coronary heart disease) and research group 3 (ischemic cerebral infarction), the method of azimuthally invariant Mueller-matrix mapping of polarization manifestations of linear birefringence of the fibrillar networks of the nerve tissue of the brain of the dead was uneffective - the strength of the method lies within an unsatisfactory level – 60% - 70%.

REFERENCES

[1]. G. Müller *et al.*, Eds., "Medical Optical Tomography: Functional Imaging and Monitoring," SPIE Press, Vol. IS11, Bellingham, Washington 1993.

[2]. L. V. Wang and H.-I. Wu. "Biomedical Optics: Principles and Imaging," Wiley-Interscience, Hoboken, New Jersey 2007.

[3]. D. Boas, C. Pitris and N. Ramanujam Eds. "Handbook of Biomedical Optics," CRC Press, Boca Raton, London, New York 2011.

[4]. T. Vo-Dinh, Ed., "Biomedical Photonics Handbook," 2nd ed., CRC Press, Boca Raton 2014.

[5]. V. V. Tuchin, "Tissue Optics: Light Scattering Methods and Instruments for Medical Diagnostics," 3rd ed., Vol. PM 254, SPIE Press, Bellingham, Washington 2015.

[6]. N. Ghosh and I. A. Vitkin. "Tissue polarimetry: concepts, challenges, applications and outlook," J. Biomed. Opt. 2011; 16: 110801.

[7]. Angelsky, O. V., Bekshaev, A. Y. A., Maksimyak, P. P., Maksimyak, A. P., & Hanson, S. G. (2018). Low-temperature laser-stimulated controllable generation of micro-bubbles in a water suspension of absorptive colloid particles. Optics Express, 26(11), 13995-14009.

[8]. Angelsky, O. V. (2007). Optical correlation techniques and applications. Optical correlation techniques and applications (pp. 1-270)

[9]. Angelsky, O. V., Ushenko, A. G., Pishak, V. P., Burkovets, D. N., Yermolenko, S. B., Pishak, O. V., & Ushenko, Y. A. (2000). Coherent introscopy of phase-inhomogeneous surfaces and layers. Paper presented at the Proceedings of SPIE - the International Society for Optical Engineering, 4016 413-418.

[10]. Angelsky OV, Bekshaev AY, Hanson SG, Zenkova CY, Mokhun II and Jun Z (2020) Structured Light: Ideas and Concepts. Front. Phys. 8:114.

[11]. Angelsky OV, Zenkova CY, Hanson SG and Zheng J (2020) Extraordinary Manifestation of Evanescent Wave in Biomedical Application. Front. Phys. 8:159.
[12]. Ushenko, Yu.A., Bachynsky, V.T., Vanchulyak, O.Ya., Dubolazov, A.V., Garazdyuk, M.S., Ushenko, V.A., "Jones-matrix mapping of complex degree of mutual anisotropy of birefringent protein networks during the differentiation of myocardium necrotic changes," (2016) Applied Optics, 55 (12), pp. B113-B119.
[13]. Ushenko, Yu.A., Dubolazov, A.V., Karachevtcev, A.O., Zabolotna, N.I., "A fractal and statistic analysis of Mueller-matrix images of phase inhomogeneous layers,"(2011) Proceedings of SPIE - The International Society for Optical Engineering, 8134, 81340P.
[14]. Ushenko, V.A., Dubolazov, A.V., "Correlation and self similarity structure of polycrystalline network biological layers Mueller matrices images," (2013) Proceedings of SPIE - The International Society for Optical Engineering, 8856.
[15]. "Cassidy, "Basic concepts of statistical analysis for surgical research," Journal of Surgical Research 128,199-206 (2005).